Improved Energy Confinement in Spheromaks with Reduced Field Errors

F. J. Wysocki, J. C. Fernández, I. Henins, T. R. Jarboe,[a] and G. J. Marklin
Los Alamos National Laboratory, Los Alamos, New Mexico 87545
(Received 15 March 1990)

An increase in the global energy confinement time (τ_E) was obtained in the CTX spheromak by replacing the high-field-error mesh-wall flux conserver with a low-field-error solid-wall flux conserver. The maximum τ_E is now 0.18 ms, an order of magnitude greater than previously reported values of $\lesssim 0.017$ ms. Both τ_E and the magnetic energy decay time (τ_W) now increase with central electron temperature, which was not previously observed. These new results are consistent with a previously proposed energy-loss mechanism associated with high edge helicity dissipation.

PACS numbers: 52.55.Hc, 52.70.Kz

A spheromak[1] is a toroidal magnetic configuration with large internal plasma currents and self-generated internal magnetic fields. This configuration has been studied for many years with the hope that it would make an attractive fusion reactor. However, an apparent condemning feature of the spheromak for reactor use was the short global energy confinement times (τ_E) previously reported,[2,3] in the 5-20-μs range. It has been proposed that the dominant energy loss has been a consequence of enhanced helicity dissipation in the edge region of the spheromak induced by magnetic-field errors.[2-4] (Helicity[5] K is the quantitative measure of the "knottedness" of magnetic-field lines, i.e., flux linkage.) In the case of CTX with a mesh-wall flux conserver,[2,6] the field errors were due to the bridges crossing the midplane gap, the coarseness of the mesh, and the nonzero resistivity of the copper rods. Edge field lines either contacted the rods themselves, or the vacuum tank surrounding the flux conserver. It was estimated that approximately 25% of the poloidal flux intersected metal, and it appears that the resistivity of the open field lines was dominated by electron-neutral collisions[2] ($\eta_{e\text{-}n}$ is much higher than $\eta_{\rm Spitzer}$ in this region). These field lines are influenced by the minimum-energy principle,[7] which states that $\lambda \equiv \mu_0 \mathbf{J}\cdot\mathbf{B}/|\mathbf{B}|^2$ (where $\mathbf{J}$ is the current density and $\mathbf{B}$ is the magnetic field) should be a spatial constant. Therefore, current is driven on the high-resistance open field lines, primarily by instabilities in the bulk plasma induced by $\nabla\lambda$. The exact nature of these instabilities is not yet understood, but it is generally accepted that they cause direct ion heating at the expense of magnetic energy (W), giving[2,3,6] ion temperatures (T_i) higher than the electron temperature (T_e). The enhanced decay rate of W (due to instabilities and direct ion heating) must be accompanied by an approximately equal helicity decay rate ($\tau_K^{-1} \equiv -\dot{K}/K$), because $W/K \propto \langle\lambda\rangle$ (volume-averaged λ), which changes only slightly with $\nabla\lambda$. Enhanced $\dot{K}$ is a direct result of large edge $\eta\mathbf{J}$, since[8] $\dot{K} \propto \int_{\rm vol} \eta\mathbf{J}\cdot\mathbf{B}\, d^3x$. (One can think of this as enhanced "untying" of the "magnetic knot" in the resistive edge.) The severe impact on τ_E came from high charge-exchange rates involving the hot, directly heated, ions.[2,3,6] Another observation consistent with edge-dominated helicity decay was that both τ_E and the global magnetic energy decay time (τ_W) did not depend on the central electron temperature.[2] Observations and conditions in other spheromak devices are also consistent with this model.[3,9]

In this Letter, we report the τ_E results from CTX with a solid-wall flux conserver specifically designed to minimize magnetic-field errors. The significantly improved confinement, now as high as 0.18 ms, the observation that both τ_W and τ_E now depend on central electron temperature, and the apparent reduction of T_i/T_e by a factor of ≈ 3 (based on the T_d measurements discussed below) are all consistent with the above model. Reduced edge volume of high $\eta\mathbf{J}$ lowers $\dot{K}$ to the point where central conditions have a significant contribution. The accompanying reduction in enhanced $\dot{W}$ reduces T_i/T_e, and τ_E is improved by the reduction of charge exchange of hot ions.

The new flux conserver, shown in Fig. 1, is cylindrical with 0.61 m radius and 0.62 m length, and has 6.4-mm-thick solid oxygen-free high-conductivity (OFHC) copper walls. All surface diagnostics (i.e., $B_{\rm wall}$ probes) are recessed in the flux conserver wall, so that the plasma "sees" a very nearly smooth surface. In addition, the midplane gap (through which most of the optical diagnostics view) was carefully designed to minimize field errors in this region. As shown in Fig. 1, the solid-copper flanges on each flux conserver half are radially extended a distance equal to the midplane gap width, and connected by 48 evenly spaced "C clamps." This ensures that the small amount of spheromak flux that bulges into the midplane gap is still relatively far from the symmetry-breaking clamps. (Note that previous solid-wall flux conservers[10] used in CTX were not designed for low field errors.) Clean discharges are obtained by depositing titanium on the plasma side of the flux conserver.[11] A small amount of bias field[12] is applied (the bias flux inside the 0.61 m radius of the flux-conserver midplane is $\lesssim 5\%$ of the spheromak poloidal flux), which was empirically found to increase the number of high-quality discharges obtainable (>25) before regettering was

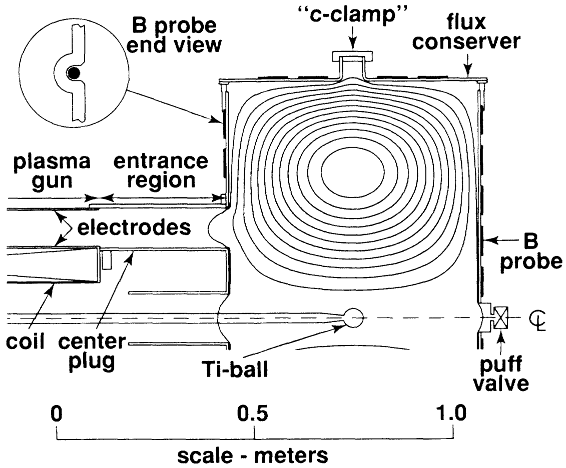

FIG. 1. The CTX low-field-error flux conserver. The entrance region, center plug, and flux conserver are all made from OFHC Cu. The electrodes are W-coated stainless steel. The Ti ball is shown in the position used for coating; it is retracted into the gun for spheromak operation. The positions of the B_{wall} probes are indicated; the seven positions to the right of the "midplane" in the figure are replicated at four torodial angles. Also indicated is the probe installation method minimizing field errors. The equilibrium shown was calculated with a typical value of bias flux.

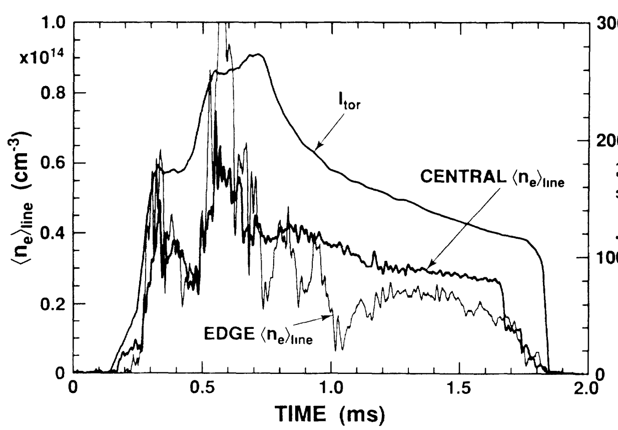

FIG. 2. A typical CTX discharge. Indicated are the toroidal plasma current as inferred from the B_{wall} data, and line-averaged electron density from the central-beam ($b=0.32$ m) and edge-beam ($b=0.54$ m) interferometer data. For this discharge, τ_E was 0.15 ms at $t=1.51$ ms.

necessary. Satomi *et al.* have used solid-wall (potentially low-field-error) flux conservers with Ti gettering,[13] but τ_E values have not been reported. The "center plug" (see Fig. 1) was first installed with the mesh-wall flux conserver, and no differences in confinement were observed for those conditions.

The CTX diagnostics include an array of 32 wall poloidal magnetic-field probes used to determine both the magnetic equilibrium and any current-driven modal activity;[14] multipoint Thomson scattering absolutely calibrated for density using Raman scattering; an eight-chord CO_2 interferometer with impact parameters (b) measured from the geometric symmetry axis ranging from 0 to 0.54 m; four bolometers for measuring radiation power; three monochromators typically used to measure time-dependent oxygen line radiation; and a polychromator for measuring impurity-ion Doppler-broadened line emission.

A typical time evolution of a low-field-error CTX discharge is shown in Fig. 2. The plasma gun is energized at $t=0$ (H_2 gas is puffed into the gun beginning at $t\approx -0.24$ ms), helicity injection begins at $t\approx 0.15$ ms, and the spheromak energy is built up and sustained[15] until $t\approx 0.7$ ms when the gun voltage is removed. Unlike previous operation, no backfill of neutral gas is used. The plasma continues to heat during the decay phase of the discharge, until the pressure gradient (∇P) becomes too large, and a ∇P-driven instability expels the central plasma[16] (at $t\approx 1.67$ ms in Fig. 2). To delay this instability as long as possible, H_2 gas is puffed at the spheromak edge (see Fig. 1 for location of the valve) to raise the edge density, thus reducing ∇P. The timing of the valve opening is adjusted so that the edge density begins to rise just prior to the typical instability time without the edge puff (at $t\approx 1.04$ ms in Fig. 2). Because the valve has a fixed plenum size, this technique is effective only in delaying the ∇P-driven instability. The long-term spheromak behavior after the instability varies. If substantial plasma density is lost, extremely rapid decay of the plasma current begins ≈ 0.1 ms later. However, the spheromak can recover (and again have high τ_E) if sufficient density remains, but repeaking of the pressure profile will eventually trigger another event. Under some conditions, no large events are observed, but many small successive events leads to a complete loss of density in ≈ 0.2 ms.

In this Letter, τ_E is reported for spheromak decay only, and τ_E would be accurately determined by $\dot{E}=-\dot{W}-E/\tau_E$, where $E=\frac{3}{2}\int_{\mathrm{vol}}(P_e+P_i)d^3x$, $P_e=n_e kT_e$, $P_i=n_i kT_i$, W is the total magnetic energy, and $-\dot{W}$ is the total input power. Radiation losses, which might be as high as 80% of $-\dot{W}$ (discussed below), have not been subtracted from the input power. It is customary to measure τ_E during a steady-state phase of the discharge where $\dot{E}\approx 0$. In the discharges considered here, no clear steady state is reached; the plasma either is in a heating phase or is suffering or recovering from a ∇P instability. Also, there are no diagnostics on CTX which can be used to estimate E as a function of time on a single discharge. A composite of Thomson scattering from many discharges is inaccurate because the data set is limited, and covers a large variation in discharge details. In this Letter, $\dot{E}$ is simply ignored, and $\tau_E \approx \frac{3}{2}\beta_{\mathrm{vol}}\tau_W$, where $\beta_{\mathrm{vol}}\equiv 2\mu_0\langle P_e+P_i\rangle_{\mathrm{vol}}/\langle B^2\rangle_{\mathrm{vol}}$ is the volume-averaged beta, and $\tau_W\equiv -W/\dot{W}$. The error introduced is estimated to be no greater than $\pm 25\%$ by noting that the inclusion of $\dot{E}$ gives $\frac{3}{2}\beta_{\mathrm{vol}}\tau_W/$

$[1+\frac{3}{2}(\beta_{vol}-\tau_W\dot{\beta}_{vol})]$, and the Thomson-scattering data indicate the "limits of plausibility" for an instantaneous $\dot{\beta}_{vol}$ as $-0.1<\dot{\beta}_{vol}<0.2\ \mathrm{ms}^{-1}$.

The value of $W(t)$ is obtained by doing a least-squares-error fit of the B_{wall} data by zero-β equilibria calculated with the linear λ model.[14] The input power is obtained by applying (in order) a 0.1-ms square-window smoothing to $W(t)$, a simple two-point time derivative, and then a second 0.1-ms square-window smoothing.

The electron contribution to β_{vol} is determined from multipoint Thomson scattering, which gives $n_e(r)$ and $T_e(r)$ for r between 0.347 and 0.560 m [see Ref. 16 for typical $P_e(r)$ profiles]. For typical equilibrium configuration, the function dV/dr vs r was calculated for $r_{mag\ axis}\le r\le r_{wall}$ along the midplane, where dV is the incremental volume between flux surfaces intersecting the midplane at r and $r+dr$, and $\langle P_e\rangle_{vol}=V^{-1}\times\int_{r_{ma}}^{r_{wall}}P_e(r)(dV/dr)dr$. Since half the volume is contained between 0.567 and 0.610 m, care must be taken in the extrapolation of P_e in this region. A linear extrapolation with the same slope as the last two data points is used (clipping at zero if this gives negative P_e), unless this slope is positive, in which case a linear extrapolation from the last point to $P_e(r_{wall})=0$ is used. The highest τ_E values reported are insensitive to these details, because the measured P_e goes to essentially zero at some $r\le 0.560$ m, and $P_e=0$ is used for larger r.

An accurate measure of the ion contribution to β_{vol} is not easily determined. The only T_i diagnostic available on CTX is a single-chord polychromator measuring Doppler-broadened impurity radiation[6] (usually O v), which gives a "temperature" (T_d). Because of the lack of spatial profiles for T_d, and the uncertainties introduced by associating T_d with the true bulk ion temperature, the assumption $T_i(x)=T_e(x)$ is made (same assumption made in Ref. 2), and $\langle P\rangle_{vol}=2\langle P_e\rangle_{vol}$. The effects of correcting τ_E based on measured T_d will be discussed below.

Figure 3 shows the obtained τ_E values vs T_e at the magnetic axis for all available multipoint Thomson-scattering data with the low-field-error flux conserver, except those data points which are less than 0.015 ms after major ∇P-driven events, or within time periods of many small successive events (eliminates five data points with $\tau_E\le 0.03$ ms). Figure 4 shows τ_W for the same set of data. These data show a clear, approximately linear dependence of both τ_E and τ_W on the central value of T_e, in extreme contrast with the data from the mesh-wall flux conserver, where no dependence was found. Comparison with Spitzer resistivity is made by defining $Z_{eff}\equiv\mu_0/2\langle\lambda\rangle^2\langle\eta^{Z=1}_{Spitzer}\rangle_{vol}\tau_W$, and using $\langle T_e^{3/2}\rangle_{vol}$ determined from the data. The Z_{eff} is <2 for 45% of the data, and <4 for 90% of the data, which is probably consistent with the impurity fraction (not measured directly).

In both figures, data which have a pressure peaking parameter ($P_{max}/\langle P\rangle_{vol}$) greater than 7 are indicated. The τ_E for this subset of data correlate with T_e, but with reduced magnitude. For these data, $\langle P\rangle_{vol}$ was calculated using $P_e=0$ in more than 55% of the volume. This may be an overly pessimistic calculation, or reduced τ_E may be a real effect associated with large ∇P_e. Note that there is no detriment to the τ_W values for these cases. Resolution of this issue is beyond the scope of this Letter.

There has been a significant reduction of T_d in the low-field-error discharges compared to the mesh-wall flux-conserver data. For mesh-wall flux-conserver discharges,[6] the only simultaneous measurements of T_d and T_e were at $t-t_s=0.3$ ms in condition 15804 from Ref. 2, giving $T_d\approx 200$ eV, $T_e\approx 30$ eV, and $T_d/T_e\approx 7$ (t_s is the time at which sustainment ends and decay be-

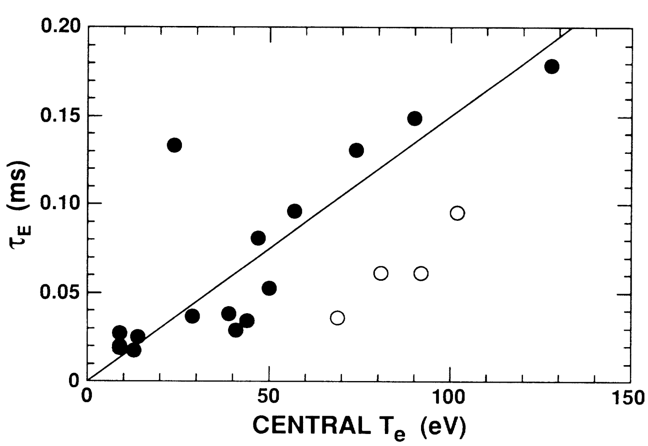

FIG. 3. The global energy confinement time for all available data with the exception of five data points (see the text). The open circles represent data with $P_{max}/\langle P\rangle_{vol}>7$. The line is a least-squares proportional fit to the solid-circle data. Radiation losses have not been subtracted from the input power.

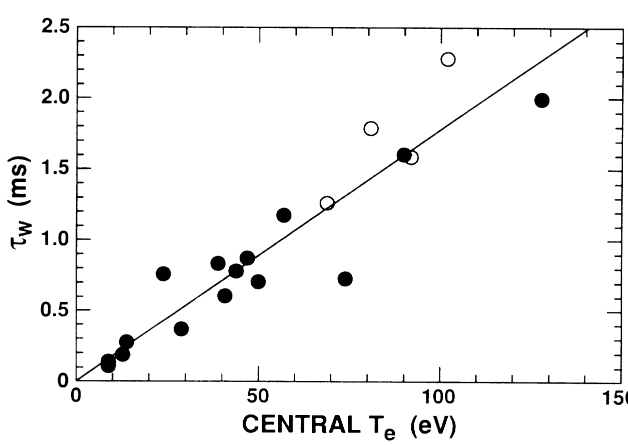

FIG. 4. The global magnetic energy decay time for the same data as Fig. 3. The line is a least-squares proportional fit to all the data.

gins). Subsequently, T_d rose to ≈ 350 eV by $t-t_s \approx 0.6$ ms, and remained approximately constant thereafter. Data from other conditions in Ref. 2 indicate that T_e increased in time, but measured values never exceeded ≈ 70–80 eV. Combined with an assumed $T_d \approx 350$ eV, it is plausible that T_d/T_e dropped in time from ≈ 7 to ≈ 4. Simultaneous measurements of T_d and T_e during decay of low-field-error discharges show a maximum T_d/T_e of ≈ 4 at $t-t_s \approx 0.4$ ms, which drops steadily to ≈ 1 by $t-t_s \approx 0.7$ ms, and stays ≈ 1 thereafter. Further interpretation of T_d is beyond the scope of this Letter.

In principle, the τ_E values should be corrected for the actual bulk ion temperature. The data discussed above give one limit; $T_i = T_e$ (divide by 2 for the limit $T_i = 0$). For another (upper) limit, the T_d value can be substituted, correcting τ_E by the factor $0.5(1+\langle n_e\rangle_{\rm vol} kT_d/\langle P_e\rangle_{\rm vol})$, which gives $\tau_E \gtrsim 0.2$ ms for 30% of the data, and a maximum τ_E of 0.26 ms. The largest corrections are for data with $\tau_E \lesssim 0.1$ ms in Fig. 3.

The substantial improvements in τ_E and τ_W indicate that enhanced edge helicity dissipation, and the accompanying consequences, have been overcome by careful design and construction of the flux conserver. The dependence of τ_W on central T_e shows the edge volume no longer dominates in determining the plasma resistance. Hot-ion charge exchange no longer dominates in determining τ_E. The bolometer data indicate that 70% to 80% of the magnetic energy dissipated before the onset of large negative $\dot{I}_{\rm tor}$ (at $t \approx 1.76$ ms in Fig. 2) appears as radiation. (The remaining magnetic energy does not appear as radiation.) Since the plasma continually heats during this time, this level of radiation loss does not represent an important limitation for the achievable plasma temperature in these discharges. Reduced radiation power would lead to a faster heating rate, and the ∇P-driven instability threshold would be reached quicker. (This instability has been observed as early as $t \approx 1.1$ ms.[16]) Only the ∇P-driven instability presently limits further heating, and thus, further increases in τ_W and τ_E. The theoretical β limits can be increased considerably by proper shaping of the spheromak boundary.[9] Experiments using a properly shaped low-field-error flux conserver are needed to further test confinement limits in spheromaks.

The authors would like to thank Robert M. Mayo for many valuable discussions. The authors acknowledge the expert technical assistance of Richard Scarberry, Robert Bollman, and Dennis Martinez. This work was supported by the Los Alamos National Laboratory Institutional Support Research fund.

[a]Present address: University of Washington, Seattle, WA 98195.

[1]M. N. Rosenbluth and M. N. Bussac, Nucl. Fusion **19**, 489 (1979).

[2]J. C. Fernández *et al.*, Nucl. Fusion **28**, 1555 (1988).

[3]R. M. Mayo *et al.*, Phys. Fluids B **2**, 115 (1990).

[4]T. R. Jarboe and B. Alper, Phys. Fluids **30**, 1177 (1987).

[5]H. K. Moffatt, J. Fluid Mech. **35**, 117 (1969).

[6]J. C. Fernández *et al.*, Nucl. Fusion **30**, 67 (1990).

[7]J. B. Taylor, Phys. Rev. Lett. **33**, 1139 (1974).

[8]J. B. Taylor, Rev. Mod. Phys. **58**, 741 (1986).

[9]M. Yamada *et al.*, in *Proceedings of the Twelfth International Conference on Plasma Physics and Controlled Nuclear Fusion Research, Nice, 1988* (IAEA, Vienna, 1989), Vol. 1, p. 539.

[10]C. W. Barnes *et al.*, Nucl. Fusion **24**, 267 (1984).

[11]T. Uyama *et al.*, Nucl. Fusion **27**, 799 (1987).

[12]C. W. Barnes *et al.*, Phys. Fluids **28**, 3443 (1985).

[13]N. Satomi *et al.*, in *Proceedings of the Eleventh International Conference on Plasma Physics and Controlled Nuclear Fusion Research, Kyoto, 1986,* edited by J. W. Weil and M. Demir (IAEA, Vienna, 1987), Vol. 2, p. 529.

[14]S. O. Knox *et al.*, Phys. Rev. Lett. **56**, 842 (1986).

[15]T. R. Jarboe *et al.*, Phys. Rev. Lett. **51**, 39 (1983).

[16]F. J. Wysocki *et al.*, Phys. Rev. Lett. **61**, 2457 (1988).